Hindawi
Wireless Communications and Mobile Computing
Volume 2018, Article ID 6310519, 13 pages
https://doi.org/10.1155/2018/6310519

Research Article

Low-Complexity Estimation for Spatially Modulated Physical-Layer Network Coding Systems

Huu Minh Nguyen,[1] Xuan Nam Tran ,[1] Van Bien Pham,[2] and Cong Dinh Nguyen[1]

[1] *Le Quy Don Technical University, Hanoi, Vietnam*
[2] *Vietnam People's Army Broadcast Center, Vietnam*

Correspondence should be addressed to Xuan Nam Tran; namtx@mta.edu.vn

Received 19 June 2018; Revised 5 September 2018; Accepted 14 September 2018; Published 1 October 2018

Academic Editor: Donatella Darsena

This paper proposes a low-complexity signal estimator at the relay node for a spatially modulated physical-layer network coding system. In the considered system, the two terminal nodes use spatial modulation to transmit their signals to the relay node during the multiple access phase. Based on the channel quantization method, we propose a low-complexity estimator which can detect both antenna indices and M-QAM symbols using successive interference cancellation (SIC). Moreover, we design signal constellations for a combined signal component at the relay for arbitrary M-QAM modulation. The obtained constellations allow further reduction of the computational complexity of the estimator. Performance evaluations show that the proposed estimator can achieve near-optimal error performance while requiring significantly less computational complexity compared with the maximum-likelihood detector, particularly with high-order modulation.

1. Introduction

Recently, two-way relay systems have received much attention [1–4] as they not only can extend system coverage but also increase transmission efficiency. Among various two-way relay schemes, physical-layer network coding (PNC) [1–5] is known as an effective scheme as it allows the two terminal nodes to transmit at the same time and same frequency during multiple access phase, thus reducing the number of exchange phases to two. As a consequence, throughput and spectral efficiency of the PNC system are higher than those of the traditional network coding (NC) [6]. However, the PNC system often requires higher complexity to obtain network coded symbols under effect of cochannel interference (CCI). This requirement leads to increase in transmission delay and energy consumption [6], which needs to be minimized for real-time applications, especially for Internet of Things (IoT) since many IoT devices are often powered by a limited-energy source such as battery. In order to perform PNC, maximum likelihood (ML) estimation was used to separate individual symbols from the two terminal nodes before combining them at the relay. Since the optimal ML estimation requires excessive complexity, especially for PNC systems with high-order QAM modulation, suboptimal estimators with less computational operations are often a better replacement.

Aiming at enhancing system performance, PNC was also proposed to combine with multiple-input multiple-output (MIMO) transmission techniques such as spatial multiplexing [7] or space-time coding [8]. However, using MIMO transmission amounts to employment of multiple radio frequency (RF) chains, causing problems in not only strict antenna synchronization but also power consumption. Spatial modulation (SM) is another MIMO technique, which can avoid these problems by activating only one antenna at a time. While enjoying this advantage SM can also increase the spectral efficiency by using the activated antenna indices to convey information bits [9, 10]. Obviously, combination of PNC and SM would provide more merits and this motivated several previous works.

1.1. Related Works. In order to improve the spectral efficiency of two-way relay systems, SM was proposed to combine with PNC in [11–14]. The work in [11] considered the combination of space-time coding spatial modulation using coordinate interleaved orthogonal designs. This scheme achieves better symbol error performance compared with the traditional network coding for both the cases in which SM is used at the relay node during the broadcast phase and at all the nodes during both the multiple access and the broadcast phase. Despite this advantage, the proposed scheme still requires high complexity due to using ML estimation for joint decoding. Moreover, this scheme cannot be applied to the two-way relay systems with more than 2 antennas at all nodes. In [10] the author proposed two spatial modulation schemes for the two-way relay channel, where either only simple SM or combined space-time coding and SM are applied at the relay node. The paper successfully derived the system capacity for both the systems in terms of achievable rate region and sum rate. The work in [12] proposed a combined SM and PNC system where simple bit-wise XOR operation was used for network coding at the relay node. Thanks to this XOR operation the proposed system can be easily extended to the case of any arbitrary number of antennas at all nodes. However, similar to that in [10], this system uses the optimal ML decoding and thus exhibits highest computational complexity. In a similar work, paper [13] proposed combining SM with PNC but adding convolutional code for error correction. The proposed scheme uses optimal ML estimation for symbol estimation and then either separate decoding or direct decoding can be employed to attain the transmitted packets from the two terminal nodes. In order to improve the error performance of the two-way relay system using network coding and spatial modulation, the work in [14] proposed using precoding with signal constellation rotation at the terminal nodes and simple XOR network coding at the relay. The proposed system with the optimized rotation angle achieves better error performance over the three-phase network coding system. However, this system needs the knowledge of channel state information (CSI) at the terminal nodes.

1.2. Contributions of the Paper. In this paper, based on the channel quantization-based SIC estimation in [4] we propose a low-complexity estimation scheme which achieves near-optimal error performance for the combined PNC and SM scheme proposed in [12]. Compared with the previous works, our main contributions can be summarized as follows:

(i) First, a new signal constellation for $x^{(sum)} = x^{(1)} + Lx^{(2)}$, where L is the channel quantization value, is proposed for arbitrary M-QAM modulated symbols $x^{(1)}$ and $x^{(2)}$. Our constellation relaxes the limitation of QPSK modulation in [4].

(ii) In order to estimate a signal point in the constellation of $x^{(sum)}$, we propose a low-complexity scheme by estimating only the positive real and imaginary parts of $x^{(sum)}$ and using a simple sign function. The complexity of the proposed estimation scheme depends less on the modulation order M but mainly the number of antennas N.

(iii) Based on the improved SIC scheme in [4], we to estimating the transmit antenna index and the M-QAM modulated symbols successively. This proposed scheme differs from those used in [10, 12, 15] in that the previous first two schemes used ML to jointly estimate both active antenna index and modulated symbols and the last scheme used QR decomposition to estimate antenna index together with an ML estimator to estimate the modulated symbols.

The rest of paper is organized as follows. Section 2 presents an overview on spatial modulation with NC using the ML estimation method. The low-complexity estimation method is discussed in details in Section 3. Section 4 analyzes the computational complexity of the proposed scheme. Performance evaluations using simulated results are shown in Section 5. Finally, Section 6 concludes the paper.

Throughout this paper, we use the following mathematical notations. Bold lower-case letter presents a vector, bold upper-case letter is used for a matrix, and italic normal letter is for a variable. $\mathbb{C}^{N\times M}$ denotes a matrix of N rows and M columns. Notations $(\cdot)^T, (\cdot)^*, |\cdot|, \|\cdot\|$ are for transpose, conjugate transpose, absolute value, and Frobenious norm, respectively.

2. Spatial Modulation with Network Coding Using ML Estimation

A typical two-way relay system using spatial modulation is illustrated in Figure 1 [12]. In this model, two terminal nodes T_1 and T_2 transmit data to each other simultaneously via a relay node R. All nodes are equipped with N, $(N = 2^K, K \geq 1)$ antennas for spatial modulation upon transmission and for signal combination upon reception. In order to implement two-way transmission, network coding by XOR mapping is used at the relay node R. Channels between each pair of transmit and receive antennas are assumed flat and slow Rayleigh fading, which are modeled by complex Gaussian distributed random variables $\sim \mathcal{N}_c(0,1)$. The signal reception at each node is affected by additive white Gaussian noise which is modeled by a complex random variable $\sim \mathcal{N}_c(0,\sigma_n^2)$.

The two-way transmission involves two phases, namely, the multiple access (MA) when T_1 and T_2 transmit their data to R and the broadcast (BC) when R forwards a network coded symbol to both T_1 and T_2.

2.1. MA Operation. In the MA phase, the two terminal nodes $T_s, (s = 1,2)$, send their $(E + C)$-length bit sequences $\mathbf{b}^{(s)}$ to R. The first $E = \log_2 N$ bits, denoted by $\mathbf{b}_{\text{id}}^{(s)} = [b_1^{(s)}, \ldots, b_E^{(s)}]^T$, are used to activate one out of N transmit antennas, while the remaining $C = \log_2 M$ bits, denoted by $\mathbf{b}_{\text{sb}}^{(s)} = [b_1^{(s)}, \ldots, b_C^{(s)}]^T$, for the M-QAM modulation. The resulting data rate is $\log_2(M \times N)$ bits/time slot. Let $u = \mathcal{M}_1(\mathbf{b}_{\text{id}}^{(1)})$ and $v = \mathcal{M}_1(\mathbf{b}_{\text{id}}^{(2)})$, where $u, v \in \{1, .., N\}$ and $\mathcal{M}_1(\cdot)$ is the mapping function which maps a bit sequence to an active antenna index; $x^{(s)} = \mathcal{M}_2(\mathbf{b}_{\text{sb}}^{(s)})$, where $\mathcal{M}_2(\cdot)$ maps a bit sequence to an M-QAM symbol. For example, the terminal node T_1 with $N = 4$ antennas needs to transmits 4 information bits 0100. Since $\mathcal{M}_1([01]) = 2$ and $\mathcal{M}_2([00]) = (1 + j)$, the second

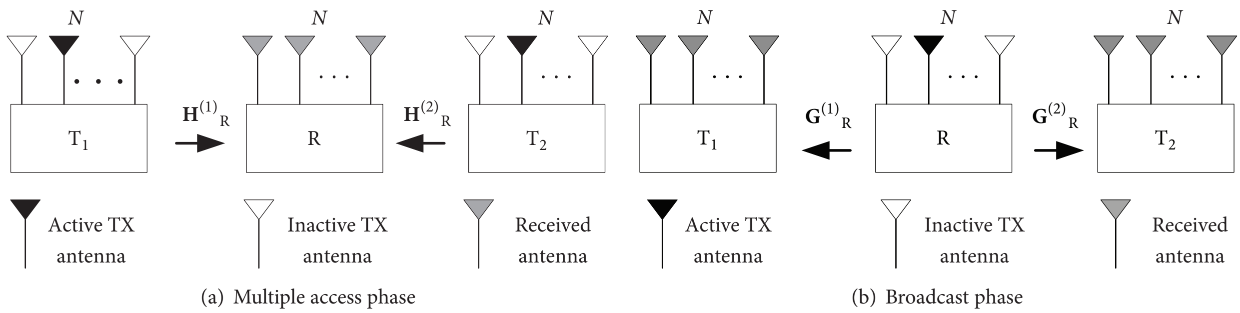

Figure 1: System model of Spatial Modulation with Network Coding for two-way relay network.

antenna is activated and the symbol $(1 + j)$ is transmitted over it.

The received signal at N antennas of R $\mathbf{y}^{(\mathrm{R})} = [y_1^{(\mathrm{R})}, .., y_N^{(\mathrm{R})}]^T$ in the MA phase is given by

$$\begin{aligned}\mathbf{y}^{(\mathrm{R})} &= \frac{1}{\sqrt{\mu}}\mathbf{h}_{uR}^{(1)}x^{(1)} + \frac{1}{\sqrt{\mu}}\mathbf{h}_{vR}^{(2)}x^{(2)} + \mathbf{n} \\ &= \overline{\mathbf{h}}_{uR}^{(1)}x^{(1)} + \overline{\mathbf{h}}_{vR}^{(2)}x^{(2)} + \mathbf{n},\end{aligned} \quad (1)$$

where $1/\sqrt{\mu}$ is a normalized power factor to ensure $\mathbb{E}(|x^{(s)}/\sqrt{\mu}|^2) = 1$; $\mathbf{n} = [n_1, \dots, n_N]^T$ denotes the thermal noise vector at N receive branches of R; $\overline{\mathbf{h}}_{iR}^{(s)} = (1/\sqrt{\mu})\mathbf{h}_{iR}^{(s)}$, $(i = u, v)$, where $\mathbf{h}_{iR}^{(s)} = [h_{i,1}^{(s)}, \cdots h_{i,N}^{(s)}]^T$ is the channel vector between the ith $(i = 1, \dots, N)$ active antenna of T_s and the N antennas of R. Assuming that the channel state information (CSI) is perfectly known at the receiver, an ML detector is used to jointly detect the transmitted symbols, including the M-QAM modulated symbols $(x^{(1)}, x^{(2)})$ and the active antenna indices (u, v) at T_s as follows [10, 12]:

$$\begin{aligned}&\left(\hat{u}, \hat{v}, \hat{x}^{(1)}, \hat{x}^{(2)}\right)_{\mathrm{ML}} \\ &\quad = \underset{\substack{(u,v)\in\{1,\dots,N\} \\ (x^{(1)},x^{(2)})\in\Omega}}{\arg\min} \left\| \mathbf{y}^{(R)} - \overline{\mathbf{h}}_{uR}^{(1)}x^{(1)} - \overline{\mathbf{h}}_{vR}^{(2)}x^{(2)} \right\|_F,\end{aligned} \quad (2)$$

where Ω denotes the M-QAM constellation. The estimated symbols are then demapped to bit sequences for network coding using XOR operation as follows:

$$\begin{aligned}\mathbf{b}_{\mathrm{id}}^{(\mathrm{R})} &= \hat{\mathbf{b}}_{\mathrm{id}}^{(1)} \oplus \hat{\mathbf{b}}_{\mathrm{id}}^{(2)} = \mathscr{M}_1^{-1}(\hat{u}) \oplus \mathscr{M}_1^{-1}(\hat{v}), \\ \mathbf{b}_{\mathrm{sb}}^{(\mathrm{R})} &= \hat{\mathbf{b}}_{\mathrm{sb}}^{(1)} \oplus \hat{\mathbf{b}}_{\mathrm{sb}}^{(2)} = \mathscr{M}_2^{-1}\left(\hat{x}^{(1)}\right) \oplus \mathscr{M}_2^{-1}\left(\hat{x}^{(2)}\right),\end{aligned} \quad (3)$$

where $\mathscr{M}_1^{-1}(\cdot)$ and $\mathscr{M}_2^{-1}(\cdot)$ are the demapping function of $\mathscr{M}_1(\cdot)$ and $\mathscr{M}_2(\cdot)$, respectively; $\oplus$ denotes the bitwise XOR operation.

2.2. BC Operation. In the BC phase, the relay node R first maps the estimated bit sequences $\mathbf{b}_{\mathrm{id}}^{(\mathrm{R})}$ and $\mathbf{b}_{\mathrm{sb}}^{(\mathrm{R})}$ to the network coded symbols that consist of the transmit antenna index of the relay node $u^{(\mathrm{R})} = \mathscr{M}_1(\mathbf{b}_{\mathrm{id}}^{(\mathrm{R})})$ and the M-QAM symbol $x^{(\mathrm{R})} = \mathscr{M}_2(\mathbf{b}_{\mathrm{sb}}^{(\mathrm{R})})$. These symbols are then broadcast to the two terminal nodes using the SM technique. The received signal at the terminal node T_s is expressed as follows:

$$\mathbf{y}^{(s)} = \frac{1}{\sqrt{\mu}}\mathbf{g}_{kS}^{(s)}x^{(\mathrm{R})} + \mathbf{z}^{(s)} = \overline{\mathbf{g}}_{kS}^{(s)}x^{(\mathrm{R})} + \mathbf{z}^{(s)}, \quad (4)$$

where $\overline{\mathbf{g}}_{kS}^{(s)} = (1/\sqrt{\mu})\mathbf{g}_{kS}^{(s)}$ and $\mathbf{g}_{kS}^{(s)} = [g_{k1}^{(s)}, \cdots, g_{kN}^{(s)}]^T$ is the channel vector between the kth $(k = 1, \dots, N)$ active antenna of R and the N antennas of T_s; $\mathbf{z}^{(s)} = [z_1^{(s)}, \cdots, z_N^{(s)}]^T$ denotes the thermal noise vector at the N receive antennas. At the terminal node T_s, an ML estimator is utilized to estimate the network coded symbols that consist of the transmit antenna index and the M-QAM symbol as follows [10, 12]:

$$\left(\hat{k}, \hat{x}^{(\mathrm{R})}\right)_{\mathrm{ML}} = \underset{\substack{k\in\{1,\dots,N\} \\ x^{(\mathrm{R})}\in\Omega}}{\arg\min} \left\| \mathbf{y}^{(s)} - \overline{\mathbf{g}}_{kS}^{(s)}x^{(\mathrm{R})} \right\|_F. \quad (5)$$

Based on the estimated network coded symbols and using its transmitted bits in the MA phase $\mathbf{b}_{\mathrm{id}}^{(s)}, \mathbf{b}_{\mathrm{sb}}^{(s)}$, each terminal node T_s can estimate the bit sequence from its counterpartner. For instance, the operation of the terminal node T_1 is given as follows:

$$\begin{aligned}\hat{\mathbf{b}}^{(2)} &= \left[\hat{\mathbf{b}}_{\mathrm{id}}^{(2)}, \hat{\mathbf{b}}_{\mathrm{sb}}^{(2)}\right] \\ &= \left[\mathscr{M}_1^{-1}\left(\hat{k}\right) \oplus \mathbf{b}_{\mathrm{id}}^{(1)}, \mathscr{M}_1^{-1}\left(\hat{x}^{(\mathrm{R})}\right) \oplus \mathbf{b}_{\mathrm{sb}}^{(1)}\right].\end{aligned} \quad (6)$$

3. Proposed Low-Complexity Estimation at Relay

Recasting (1) in the matrix form, we have

$$\mathbf{y}^{(\mathrm{R})} = \overline{\mathbf{H}}_{(u,v)}\mathbf{x} + \mathbf{n}, \quad (7)$$

where

$$\begin{aligned}\overline{\mathbf{H}}_{(u,v)} &= \begin{bmatrix} \overline{h}_{u1}^{(1)} & \overline{h}_{v1}^{(2)} \\ \vdots & \vdots \\ \overline{h}_{uN}^{(1)} & \overline{h}_{vN}^{(2)} \end{bmatrix}, \\ \mathbf{x} &= \left[x^{(1)} \quad x^{(2)}\right]^T.\end{aligned} \quad (8)$$

The channel matrix $\overline{\mathbf{H}}_{(u,v)}$ in (7) can be decomposed using a QR factorization as follows:

$$\overline{\mathbf{H}}_{(u,v)} = \overline{\mathbf{Q}}_{(u,v)}\overline{\mathbf{R}}_{(u,v)}, \tag{9}$$

where $\overline{\mathbf{Q}}_{(u,v)}$ is a unitary matrix with $\overline{\mathbf{Q}}^H_{(u,v)}\overline{\mathbf{Q}}_{(u,v)} = \mathbf{I}^{N\times N}$ and $\mathbf{I}^{N\times N} \in \mathbb{C}^{N\times N}$ and $\overline{\mathbf{R}}_{(u,v)} = \begin{bmatrix} \mathbf{R}^{2\times 2}_{(u,v)} \\ \mathbf{0}^{(N-2)\times 2} \end{bmatrix}$ is an upper triangle matrix, where $\mathbf{R}^{2\times 2}_{(u,v)} = \begin{bmatrix} r^{(1,1)}_{(u,v)} & r^{(1,2)}_{(u,v)} \\ 0 & r^{(2,2)}_{(u,v)} \end{bmatrix}$ with $r^{(i,i)}_{(u,v)}$, $(i = 1, 2)$ being a real number and $r^{(1,2)}_{(u,v)}$ a complex number. Multiplying both sides of (7) by $\overline{\mathbf{Q}}^H_{(u,v)}$ gives us

$$\overline{\mathbf{w}}_{(u,v)} \triangleq \overline{\mathbf{Q}}^H_{(u,v)}\mathbf{y}^{(\mathrm{R})} = \begin{bmatrix} \mathbf{R}^{2\times 2}_{(u,v)} \\ \mathbf{0}^{(N-2)\times 2} \end{bmatrix}\mathbf{x} + \overline{\mathbf{n}}, \tag{10}$$

where $\overline{\mathbf{n}} = [\overline{n}_1, \ldots, \overline{n}_N]^T \triangleq \overline{\mathbf{Q}}^H_{(u,v)}\mathbf{n}$.

Therefore, the ML estimation applied to (10) can be expressed as follows [16]:

$$\left(\widehat{u}, \widehat{v}, \widehat{x}^{(1)}, \widehat{x}^{(2)}\right)_{\mathrm{ML}} = \underset{\substack{(u,v)\in\{1,\ldots,N\} \\ (x^{(1)},x^{(2)})\in\Omega}}{\arg\min} \left\| \overline{\mathbf{w}}_{(u,v)} - \overline{\mathbf{R}}_{(u,v)}\mathbf{x} \right\|_F . \tag{11}$$

It is worth noting that in order to perform ML estimation in (2) or (11), the required computational complexity is $N^2 \times M^2$. The larger the size of the signal constellation is, the more estimation complexity it requires. As a consequence, this results in increased transmission delay and large consumed energy for processing.

3.1. Proposed Low-Complexity Estimation Using SM-QSIC. In this section, we propose a low-complexity estimation method by combining the channel quantization and the SIC technique, abbreviated as SM-QSIC. The proposed method consists of two stages, namely, channel quantization and SIC-based estimation, as follows.

3.1.1. Channel Quantization. Because $\overline{\mathbf{R}}_{(u,v)}$ has only the first non-zero two rows, the first two elements of $\overline{\mathbf{w}}_{(u,v)}$ in (10) can be rewritten as follows:

$$\begin{aligned} w^{(1)}_{(u,v)} &= r^{(1,1)}_{(u,v)}x^{(1)} + r^{(1,2)}_{(u,v)}x^{(2)} + \overline{n}_1, \\ w^{(2)}_{(u,v)} &= r^{(2,2)}_{(u,v)}x^{(2)} + \overline{n}_2. \end{aligned} \tag{12}$$

To simplify the presentation the subscripts (u, v) will be omitted in the following parts. $w^{(1)}$ in (12) can be decomposed as follows:

$$\begin{aligned} w^{(1)} = r^{(1,1)}\left(x^{(1)} + Lx^{(2)}\right) + r^{(1,1)}\left(\frac{r^{(1,2)}}{r^{(1,1)}} - L\right)x^{(2)} \\ + \overline{n}_1. \end{aligned} \tag{13}$$

Let L denote the quantization level such that $L = \mathrm{round}(r^{(1,2)}/r^{(1,1)})$, where round(·) denotes the rounding operation. $l \triangleq r^{(1,2)}/r^{(1,1)} - L$ is regarded as the deviation between L and $r^{(1,2)}/r^{(1,1)}$. It is also often referred to as quantization error or residual interference.

Denoting $x^{(\mathrm{sum})} \triangleq x^{(1)} + Lx^{(2)}$, (12) can be rewritten as follows:

$$\begin{aligned} w^{(1)} &= r^{(1,1)}x^{(\mathrm{sum})} + r^{(1,1)}lx^{(2)} + \overline{n}_1, \\ w^{(2)} &= r^{(2,2)}x^{(2)} + \overline{n}_2. \end{aligned} \tag{14}$$

Using the SIC estimation $x^{(2)}$ is first estimated from $w^{(2)}$. Then $x^{(\mathrm{sum})}$ can be detected by removing the interference component $x^{(2)}$ in $w^{(1)}$. In fact, to estimate $x^{(\mathrm{sum})}$, its constellation must be stored in advance at the receiver. In order to limit memory size for storing the constellation of $x^{(\mathrm{sum})}$, we derive the following lemma.

Lemma 1. *If* $|r^{(1,1)}| \geq |r^{(1,2)}|$, *$L$ belongs to the set* $\{0, \pm 1, \pm j, \pm 1 \pm j\}$.

Proof. Because $r^{(1,1)}$ is a real and $r^{(1,2)} = r^{(1,2)}_r + jr^{(1,2)}_i$ is a complex number, where $j^2 = -1$, from the above assumptions, we have $(r^{(1,2)}_r/r^{(1,1)})^2 + (r^{(1,2)}_i/r^{(1,1)})^2 \leq 1$ or $|r^{(1,2)}_r/r^{(1,1)}| \leq 1$ and $|r^{(1,2)}_i/r^{(1,1)}| \leq 1$. Moreover, $L = L_r + jL_i = \mathrm{round}(r^{(1,2)}/r^{(1,1)}) = \mathrm{round}(r^{(1,2)}_r/r^{(1,1)}) + j\mathrm{round}(r^{(1,2)}_i/r^{(1,1)})$. This means that $L_r, L_i \in \{0, \pm 1\}$, or $L \in \{0, \pm 1, \pm j, \pm 1 \pm j\}$.

On the other hand, from (14), it can be seen that estimation reliability of $x^{(\mathrm{sum})}$ depends on $|l|^2$. Therefore, we propose an effective algorithm (Algorithm 1) to satisfy the condition $L \in \{0, \pm 1, \pm j, \pm 1 \pm j\}$ and reduce the magnitude of $|l|^2$. □

3.1.2. SIC-Based Estimation. This estimation method involves two steps: estimation of the active antenna index and estimation of the M-QAM modulated symbol.

(i) Estimation of the Active Antenna Index

Step 1. Soft estimation of $x^{(2)}$ in the second equation of (14) using $w^{(2)}$.

(i) For the 4-QAM constellation, the soft estimation is done as follows [17]:

$$\overline{x}^{(2)} = \mathbb{E}\left\{x^{(2)} \mid w^{(2)}\right\} = \tanh\left(\frac{r^{(2,2)}w^{(2)}}{\sigma_n^2}\right). \tag{15}$$

(ii) For other cases, i.e., $M > 4$, the soft estimation is given by [18]

$$\overline{x}^{(2)} = \begin{cases} \mathrm{sign}\left(\dfrac{w^{(2)}}{r^{(2,2)}}\right)\left(\sqrt{M} - 1\right) & \text{if } \left|\dfrac{w^{(2)}}{r^{(2,2)}}\right| > \left(\sqrt{M} - 1\right), \\ \dfrac{w^{(2)}}{r^{(2,2)}} & \text{if } \left|\dfrac{w^{(2)}}{r^{(2,2)}}\right| \leq \left(\sqrt{M} - 1\right). \end{cases} \tag{16}$$

Note that the estimation in (15) and (16) is performed separately for the real and imaginary parts.

Input: $N, (u,v) \in \{1,\ldots,N\}, \overline{\mathbf{H}}_{(u,v)} \in \mathbb{C}^{N\times 2}, \mathbf{y}^{(\mathrm{R})} \in \mathbb{C}^{N\times 1}$
Initialization: $\overline{\mathbf{w}}_{(u,v)} \in \mathbb{C}^{N\times 1}, \overline{\mathbf{Q}}_{(u,v)} \in \mathbb{C}^{N\times N}, \overline{\mathbf{R}}_{(u,v)} \in \mathbb{C}^{N\times 2}, L_{(u,v)}, l_{(u,v)} \in \mathbb{Z}$
Decompose channel matrix $\overline{\mathbf{H}}_{(u,v)}$: $[\overline{\mathbf{Q}}_1, \overline{\mathbf{R}}_1] = \mathrm{qr}(\overline{\mathbf{H}}_{(u,v)})$
Exchange 2 columns of $\overline{\mathbf{H}}_{(u,v)}$ to get $\overleftarrow{\mathbf{H}}_{(u,v)}$ and decompose it: $[\overline{\mathbf{Q}}_2, \overline{\mathbf{R}}_2] = \mathrm{qr}(\overleftarrow{\mathbf{H}}_{(u,v)})$
Calculate quantization values: $L_1 = \mathrm{round}(r_1^{(1,2)}/r_1^{(1,1)}), L_2 = \mathrm{round}(r_2^{(1,2)}/r_2^{(1,1)})$
Calculate residual interference: $l_1 = r_1^{(1,2)}/r_1^{(1,1)} - L_1, l_2 = r_2^{(1,2)}/r_2^{(1,1)} - L_2$
If $|L_1| \le \sqrt{2}$ and $|L_2| \le \sqrt{2}$ then
  If $|l_1| \le |l_2|$ then
    $\overline{\mathbf{Q}}_{(u,v)} = \overline{\mathbf{Q}}_1, \overline{\mathbf{R}}_{(u,v)} = \overline{\mathbf{R}}_1, L_{(u,v)} = L_1, l_{(u,v)} = l_1$
  Else
    $\overline{\mathbf{Q}}_{(u,v)} = \overline{\mathbf{Q}}_2, \overline{\mathbf{R}}_{(u,v)} = \overline{\mathbf{R}}_2, L_{(u,v)} = L_2, l_{(u,v)} = l_2$
  End
Else if $|L_1| \le \sqrt{2}$
  $\overline{\mathbf{Q}}_{(u,v)} = \overline{\mathbf{Q}}_1, \overline{\mathbf{R}}_{(u,v)} = \overline{\mathbf{R}}_1, L_{(u,v)} = L_1, l_{(u,v)} = l_1$
Else
  $\overline{\mathbf{Q}}_{(u,v)} = \overline{\mathbf{Q}}_2, \overline{\mathbf{R}}_{(u,v)} = \overline{\mathbf{R}}_2, L_{(u,v)} = L_2, l_{(u,v)} = l_2$
End
Calculate $\overline{\mathbf{w}}_{(u,v)} = \overline{\mathbf{Q}}_{(u,v)}^H \mathbf{y}^{(\mathrm{R})}$
Output: $\overline{\mathbf{w}}_{(u,v)}, \overline{\mathbf{R}}_{(u,v)}, L_{(u,v)}, l_{(u,v)}$

Algorithm 1: Matrix decomposition and quantization value calculation.

Step 2. Cancel the residual interference $lx^{(2)}$ in (14) to estimate the signal $x^{(\mathrm{sum})}$. Using the conventional SIC, the estimate of $x^{(2)}$ in (1), denoted by $\widehat{x}^{(2)}$, is used to remove the noise components $r^{(1,2)}x^{(2)}$ in (12) before estimating $x^{(1)}$. If the estimate $\widehat{x}^{(2)}$ is correct, the noise component $r^{(1,2)}x^{(2)}$ is removed and it does not affect the estimation of $x^{(1)}$. In contrast, if the estimate $\widehat{x}^{(2)}$ is erroneous, the removal of $r^{(1,2)}x^{(2)}$ results in an additional interference component $r^{(1,2)}\widehat{x}^{(2)}$ which affects the estimation of $x^{(1)}$ significantly. The larger $|r^{(1,2)}|^2$, the more significant the impact of this interference. In order to lessen this impact, instead of complete removing $r^{(1,2)}x^{(2)}$, we use the SIC method in [4] to remove only a part of it, namely, $lx^{(2)}$ as follows.

Let us define

$$\begin{aligned} w^{(1a)} &\triangleq \frac{w^{(1)}}{r^{(1,1)}} = x^{(\mathrm{sum})} + lx^{(2)} + \frac{\overline{n}_1}{r^{(1,1)}}, \\ w^{(1b)} &\triangleq w^{(1a)} - l\overline{x}^{(2)} = x^{(\mathrm{sum})} + l\left(x^{(2)} - \overline{x}^{(2)}\right) + \frac{\overline{n}_1}{r^{(1,1)}}. \end{aligned} \tag{17}$$

The decision function of $\widetilde{x}^{(\mathrm{sum})}$ is given by

$$\widetilde{x}^{(\mathrm{sum})} = \widehat{Q}\left(w^{(1b)}\right), \tag{18}$$

where $\widehat{Q}$ is the decision function for the signal constellation $(x^{(1)} + Lx^{(2)})$. Details on this decision function will be presented in the next part.

Step 3. Remove $x^{(\mathrm{sum})}$ and estimate $x^{(2)}$ using the maximum ratio combining (MRC) as follows:

$$\widetilde{x}^{(2)} = \mathrm{Q}\left(\frac{l^*\left(w^{(1a)} - \widetilde{x}^{(\mathrm{sum})}\right) + r^{(2,2)}w^{(2)}}{|l|^2 + \left(r^{(2,2)}\right)^2}\right). \tag{19}$$

Step 4. Calculate the estimation error and detect the active antenna index of the terminals. The estimation error of $(\widetilde{x}_{(u,v)}^{(\mathrm{sum})}, \widetilde{x}_{(u,v)}^{(2)})$ can be calculated as follows:

$$\Delta_{(\widetilde{\mathbf{x}}_{(u,v)}^{(\mathrm{sum})})} = \left\|\overline{\mathbf{w}}_{(u,v)} - \overline{\mathbf{R}}_{(u,v)}^{(\mathrm{sum})}\widetilde{\mathbf{x}}_{(u,v)}^{(\mathrm{sum})}\right\|_F, \tag{20}$$

where

$$\begin{aligned} \overline{\mathbf{R}}_{(u,v)}^{(\mathrm{sum})} &= \begin{bmatrix} \mathbf{R}_{(u,v)}^{(\mathrm{sum})(2\times 2)} \\ \mathbf{0}^{(N-2)\times 2} \end{bmatrix}, \\ \mathbf{R}_{(u,v)}^{(\mathrm{sum})(2\times 2)} &= \begin{bmatrix} r_{(u,v)}^{(1,1)} & r_{(u,v)}^{(1,1)} l_{(u,v)} \\ 0 & r_{(u,v)}^{(2,2)} \end{bmatrix}, \\ \widetilde{\mathbf{x}}_{(u,v)}^{(\mathrm{sum})} &= \left[\widetilde{x}_{(u,v)}^{(\mathrm{sum})} \quad \widetilde{x}_{(u,v)}^{(2)}\right]^T. \end{aligned} \tag{21}$$

Finally, a pair of active antenna indices is detected as follows:

$$(\widehat{u}, \widehat{v})_{\mathrm{ML}} = \min_{(u,v)\in\{1,\ldots,N\}} \left\{\Delta_{(\widetilde{\mathbf{x}}_{(u,v)}^{(sum)})}\right\} \tag{22}$$

(ii) Estimation of the M-QAM Modulated Symbol

The total estimation of $x^{(1)}$ and $x^{(2)}$ from the received signal in (12) is performed as follows.

Step 1. Estimate the modulated symbol $x^{(1)}$ in the M-QAM constellation. Cancel $x^{(2)}$ in $w_{(\widehat{u},\widehat{v})}^{(1)}$ in (12) to estimate the modulated symbol $x^{(1)}$. Different from the conventional SIC method which uses the estimate $\widetilde{x}_{(\widehat{u},\widehat{v})}^{(2)}$ obtained from $w_{(\widehat{u},\widehat{v})}^{(2)}$ in

(12), our scheme uses the estimate $\tilde{x}^{(2)}_{(\hat{u},\hat{v})}$ from the MRC in (19) as follows:

$$\hat{x}^{(1)} = Q\left(\frac{w^{(1)}_{(\hat{u},\hat{v})} - r^{(1,2)}_{(\hat{u},\hat{v})}\tilde{x}^{(2)}_{(\hat{u},\hat{v})}}{r^{(1,1)}_{(\hat{u},\hat{v})}}\right). \quad (23)$$

Step 2. Estimate the modulated symbol $x^{(2)}$. In (19), we only estimate a part of the signal $x^{(2)}$. Therefore, the total estimation of the modulated symbol $x^{(2)}$ in the received signal can be estimated as follows:

$$\hat{x}^{(2)} = Q\left(\frac{r^{(1,2)*}_{(\hat{u},\hat{v})}\left(w^{(1)}_{(\hat{u},\hat{v})} - r^{(1,1)}_{(\hat{u},\hat{v})}\hat{x}^{(1)}\right) + r^{(2,2)}_{(\hat{u},\hat{v})}w^{(2)}_{(\hat{u},\hat{v})}}{\left|r^{(1,2)}_{(\hat{u},\hat{v})}\right|^2 + \left(r^{(2,2)}_{(\hat{u},\hat{v})}\right)^2}\right). \quad (24)$$

Similar to [12], the pair of active antennas $(\hat{u},\hat{v})$ and the pair of M-QAM modulated symbols $(\hat{x}^{(1)},\hat{x}^{(2)})$ will be mapped to network coded symbols. Then the relay uses spatial modulation to broadcast these symbols to the two terminal nodes as in Section 2.

3.2. Constellation Design for $(x^{(1)} + Lx^{(2)})$ and Decision Function $\widehat{Q}(\cdot)$. To decide the signal $x^{(\text{sum})}$ in (18), we first study the constellation of the signal $x^{(\text{sum})}$ and then create a decision rule for the function $\widehat{Q}(\cdot)$. Because of limited space, we only focus our presentation on the case with $M \le 64$. The remaining case with $M > 64$ can be extended in a straightforward way.

3.2.1. Constellation Design for $(x^{(1)} + Lx^{(2)})$. It can be seen from the above section that L belongs to one of the values: $\{0, \pm 1, \pm j, \pm 1 \pm j\}$. Meanwhile, the signals $x^{(1)}$ and $x^{(2)}$ belong to the M-QAM constellation. Therefore, the constellation of the signal $(x^{(1)} + Lx^{(2)})$ can be described for various values of L and M as shown in Figures 2, 3, and 4.

3.2.2. Proposed Decision Function $\widehat{Q}(\cdot)$. Since $L \in \{0, \pm 1, \pm j, \pm 1 \pm j\}$, the decision function $\widehat{Q}(\cdot)$ is performed as follows:

(a) Case $L \in \{0, \pm 1, \pm j\}$: Because the M-QAM constellation is square, we can perform separate estimation for the real part and the imaginary part of the signal $(x^{(1)} + Lx^{(2)})$ to reduce complexity when estimating this signal. On the other hand, because the constellation is symmetric, we only need to estimate signal points in the first quarter of the constellation using the sign function. The decision function $\widehat{Q}(\cdot)$ in (18) is given by

$$\begin{aligned}\tilde{x}^{(\text{sum})} &= \widehat{Q}\left(w^{(1b)}\right) \\ &= \widehat{Q}\left(x^{(\text{sum})} + l\left(x^{(2)} - \overline{x}^{(2)}\right) + \frac{n^{(1)}}{r^{(1,1)}}\right) \quad (25) \\ &= \text{sign}\left(w^{(1b)}_r\right)\hat{x}^{(\text{sum})}_r + j\text{sign}\left(w^{(1b)}_i\right)\hat{x}^{(\text{sum})}_i,\end{aligned}$$

where sign$(\cdot)$ represents the sign function and x_r, x_i denote the real and imagine part of the complex variable x, respectively. The real and the imaginary part of $\hat{x}^{(\text{sum})}$ are determined as follows:

$$\begin{aligned}\hat{x}^{(\text{sum})}_r &= \underset{x^{(\text{sum})}_r \in \mathscr{A}}{\arg\min}\left|\left|w^{(1b)}_r\right| - x^{(\text{sum})}_r\right|, \\ \hat{x}^{(\text{sum})}_i &= \underset{x^{(\text{sum})}_i \in \mathscr{A}}{\arg\min}\left|\left|w^{(1b)}_i\right| - x^{(sum)}_i\right|,\end{aligned} \quad (26)$$

where $\mathscr{A}$ is the set of values for different M and L as given in Table 1. Notice that, in the case $M = 4$, $L = 0$ we can select $\hat{x}^{(\text{sum})}_r = \hat{x}^{(\text{sum})}_i = 1$.

Let us consider the simple case with $M = 16$ and $L = 0$ and assume that we need to estimate $(w^{(1b)}_r, w^{(1b)}_i)$. The estimation values correspond to the point $C_1(-1.5, -1.5)$ as illustrated in Figure 5. For the ML estimation, there are a total of 16 calculations to decide the point $C_1(-1.5, -1.5)$ to the constellation point $(-1, -1)$. If we estimate the real and the imagine part, separately, then it reduces to 8 calculations. Meanwhile, our proposed method only needs 4 calculations to obtain the magnitude and 1 calculation to decide the sign. The more M increases, the more the complexity can be reduced compared with that of the conventional estimation methods.

(b) Case $L \in \{\pm 1 \pm j\}$: It can be seen from Figures 2(c), 3(c), and 4(c) that the constellation is truncated at all four quadrants. At the first quadrant, the constellation is bounded by a line $x_r + x_i - 4 = 0$ when $M = 4$ and $x_r + x_i - 12 = 0$, when $M = 16$ and $x_r + x_i - 28 = 0$, and when $M = 64$, where x_r, x_i, respectively, represents the arbitrary real and imaginary values that satisfy the zero condition of the equation. Therefore, in the case $L \in \{\pm 1 \pm j\}$ we can perform estimation in two steps as follows.

Step 1 (decide estimation domain). The signal points $(|w^{(1b)}_r|, |w^{(1b)}_i|)$ are determined to the right or to the left of the boundary line as given

$$\mathit{Estimation\_domain} = \begin{cases}\text{right} & \text{if } \left(\left|w^{(1b)}_r\right| + \left|w^{(1b)}_i\right| - a\right) > 0, \\ \text{left} & \text{if } \left(\left|w^{(1b)}_r\right| + \left|w^{(1b)}_i\right| - a\right) \le 0,\end{cases} \quad (27)$$

where $a = -4$ if $M = 4$ and $a = -12$ and $a = -28$ if $M = 16$ and $M = 64$, respectively.

Step 2 (estimation). (i) If *Estimation_domain* is on the left of the boundary line $x_r + x_i - a = 0$, the estimation function is same as the case $L \in \{0, \pm 1, \pm j\}$. However, the set of $\mathscr{A}$ in (26) is taken from Table 2.

(ii) If *Estimation_domain* is on the right of the boundary line $x_r + x_i - a = 0$; at this point, we only need to estimate the points on the boundary line as follows:

$$\hat{x}^{(\text{sum})} = \underset{x^{(\text{sum})} \in \mathscr{B}}{\arg\min}\left|\left|w^{(1b)}\right| - x^{(\text{sum})}\right|^2, \quad (28)$$

where $\mathscr{B}$ is the set of points on the boundary line as given in the Table 3. Finally, substitute $\hat{x}^{(\text{sum})}$ into (25) to get $\tilde{x}^{(\text{sum})}$.

4. Complexity Analysis

In order to show the advantage of the proposed method in terms of computational complexity, we estimate the floating

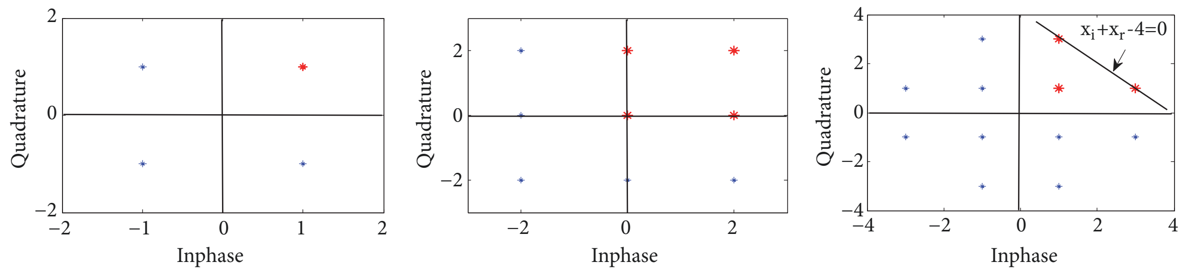

(a) $L = 0$ (b) $L \in \{\pm 1, \pm j\}$ (c) $L \in \{\pm 1 \pm j\}$

FIGURE 2: Signal constellation of $(x^{(1)} + Lx^{(2)})$ for $M = 4, L \in \{0, \pm 1, \pm j, \pm 1 \pm j\}$.

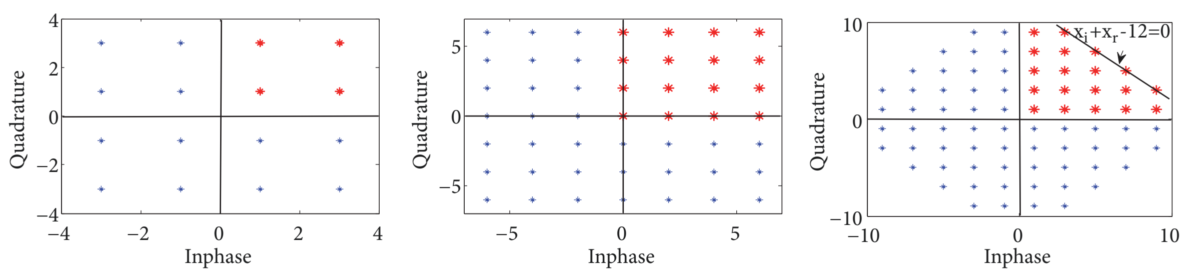

(a) $L = 0$ (b) $L \in \{\pm 1, \pm j\}$ (c) $L \in \{\pm 1 \pm j\}$

FIGURE 3: Signal constellation of $(x^{(1)} + Lx^{(2)})$ for $M = 16, L \in \{0, \pm 1, \pm j, \pm 1 \pm j\}$.

point operations (flop). Similar to [19], all real algebraic operation is considered as 1flop, a complex multiplication 6flops, a complex division 11flops, and a complex addition or subtraction 2flops.

4.1. Complexity of Decision Functions $\widehat{Q}(\cdot)$ *and* $Q(\cdot)$. First we analyze the complexity of the decision function $Q(\cdot)$ in (18). From the above section, it can be seen that, for a certain modulation order M, the signal $(x^{(1)} + Lx^{(2)})$ belongs only to one of three constellations corresponding to $L = 0$, $L \in \{\pm 1, \pm j\}$, or $L \in \{\pm 1 \pm j\}$. Therefore, the probability of $(x^{(1)} + Lx^{(2)})$ falls into one of the three constellations that can be given by

$$\begin{aligned} \mathrm{P_r}\left(L = \mathrm{round}\left(\frac{r^{(1,2)}}{r^{(1,1)}}\right)\right) &= \mathrm{P_r}\left(L \in \{0\}\right) + \mathrm{P_r}\left(L \in \{\pm 1, \pm j\}\right) \\ &\quad + P_r\left(L \in \{\pm 1 \pm j\}\right) = 1, \end{aligned} \tag{29}$$

where $\mathrm{P_r}(L \in \{0\}) = \mathrm{P_r}(L \in \{\pm 1, \pm j\}) = \mathrm{P_r}(L \in \{\pm 1 \pm j\}) = 1/3$.

(a) Case $L \in \{\pm 1 \pm j\}$, because the complexity of function $\widehat{Q}(\cdot)$ when $L \in \{\pm 1 \pm j\}$ varies depending on the value $(|w_r^{(1b)}|, |w_i^{(1b)}|)$ lying on the left or on the right of the boundary. Therefore, in this case the complexity is given as an average value based on the probability that the received signal lying on the right or left side of the boundary. Assuming that the probability that $(w_r^{(1b)}, w_i^{(1b)})$ lying close to an arbitrary constellation point of the square constellation (not blocked by the boundary) is the same. Letting $\Phi = |w_r^{(1b)}| + |w_i^{(1b)}| - a$, based on the geometric area we can determine the probability that the received signal lying on the right side of the boundary $P_r(\Phi > 0)_M$ and the probability of the remaining points $\mathrm{P_r}(\Phi \leq 0)_M = 1 - \mathrm{P_r}(\Phi > 0)_M$ as shown in Figure 6. These probabilities are presented in Table 4.

$\mathcal{A}_{M,\overline{L}}$ is an average value of the set $\mathcal{A}$ over L at a certain value of M, and $\mathcal{B}_M$ is the sum of the values of the set $\mathcal{B}$. The values of $\mathcal{A}_{M,\overline{L}}$ and $\mathcal{B}_M$ are summarized in Table 5.

(i) If $|w_r^{(1b)}| + |w_i^{(1b)}| - a > 0$, the complexity of the decision function $\widehat{Q}(\cdot)$ in (28) is $5\mathcal{B}_M$ flops.

(ii) If $|w_r^{(1b)}| + |w_i^{(1b)}| - a \leq 0$, the total complexity of the decision function $\widehat{Q}(\cdot)$ in (25) and (26) is $(4 + 6\mathcal{A}_{M,\overline{L}})$ flops.

Therefore, the average complexity of the decision function $\widehat{Q}(\cdot)$ for $L \in \{\pm 1 \pm j\}$ is given by

$$\begin{aligned} &4 + \mathrm{P_r}\left(\Phi \leq 0\right)_M \times \left(4 + 6\mathcal{A}_{M,\overline{L}}\right) + \mathrm{P_r}\left(\Phi > 0\right)_M \\ &\quad \times \left(5\mathcal{B}_M\right) \text{ flops.} \end{aligned} \tag{30}$$

(b) Case $L = 0$ or $L \in \{\pm 1, \pm j\}$: The total complexity of the decision function $\widehat{Q}(\cdot)$ in (25) and (26) is $(4 + 6\mathcal{A}_{M,\overline{L}})$ flops. Notice that the complexity of the decision function $Q(\cdot)$ is equal to that of the function $\widehat{Q}(\cdot)$ when $L = 0$.

The overall average complexity when using the function $\widehat{Q}(\cdot)$ to estimate the signal $x^{(\mathrm{sum})}$ with all values $L \in \{0, \pm 1, \pm j, \pm 1 \pm j\}$ is then given by

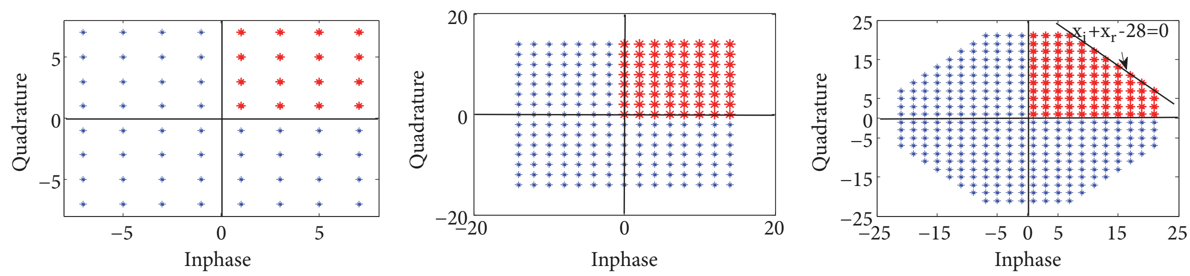

(a) $L = 0$ (b) $L \in \{\pm 1, \pm \mathrm{j}\}$ (c) $L \in \{\pm 1 \pm \mathrm{j}\}$

FIGURE 4: Signal constellation of $(x^{(1)} + Lx^{(2)})$ for $M = 64$, $L \in \{0, \pm 1, \pm j, \pm 1 \pm j\}$.

TABLE 1: Value sets of $\mathscr{A}$ when $L \in \{0, \pm 1, \pm j\}$.

	$M = 4$		$M = 16$		$M = 64$	
	$L = 0$	$L \in \{\pm 1, \pm j\}$	$L = 0$	$L \in \{\pm 1, \pm j\}$	$L = 0$	$L \in \{\pm 1, \pm j\}$
$\mathscr{A}$	$\{1\}$	$\{0, 2\}$	$\{1, 3\}$	$\{0, 2, 4, 6\}$	$\{1, 3, 5, 7\}$	$\{0, 2, 4, 6, 8, 10, 12, 14\}$

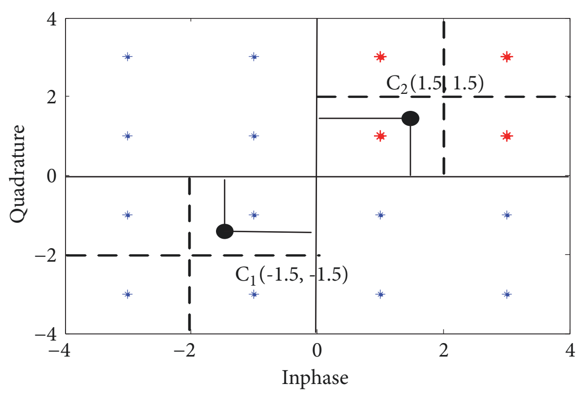

FIGURE 5: Illustrated example for which $(w_r^{(1b)}, w_i^{(1b)})$ belongs to the point $C_1(-1.5, -1, 5)$ and $(|w_r^{(1b)}|, |w_i^{(1b)}|)$ belongs to $C_2(1.5, 1, 5)$ on the constellation $(x^{(1)} + Lx^{(2)})$ with $M = 16$ and $L = 0$.

TABLE 2: The value sets of $\mathscr{A}$ according to M when $L \in \{\pm 1 \pm j\}$, *Estimation_domain* is on the left of the boundary.

	$M = 4$	$M = 16$	$M = 64$
$\mathscr{A}$	$\{1, 3\}$	$\{1, 3, 5, 7, 9\}$	$\{1, 3, 5, 7, 9, 11, 13, 15, 17, 19, 21\}$

$$\begin{aligned} C_{\widehat{Q}(\cdot)} &= \frac{2}{3}\left(4 + 6\mathscr{A}_{M,\overline{L}}\right) + \frac{1}{3}\left(4 + P_r(\Phi \le 0)_M\left(4\right.\right. \\ &\quad \left.\left. + 6\mathscr{A}_{M,\overline{L}}\right) + P_r(\Phi > 0)_M\left(5\mathscr{B}_M\right)\right) \\ &= \left(\frac{1}{3}\left(P_r(\Phi \le 0)_M\left(4 + 6\mathscr{A}_{M,\overline{L}}\right)\right.\right. \\ &\quad \left.\left. + 5P_r(\Phi > 0)_M\mathscr{B}_M\right) + 4\mathscr{A}_{M,\overline{L}} + 4\right) \text{ flops.} \end{aligned} \tag{31}$$

The complexity of function $\widehat{Q}(\cdot)$ and $Q(\cdot)$ according to M flops is summarized in Table 6.

4.2. Complexity of Related Estimation Methods. According to [19], the number of flops required for decomposing the matrix $\mathbf{H}_{(u,u)}$ of size $N \times 2$ is $(16N^2 + 12N)$ flops. The number of flops required for multiplying $\mathbf{Q}_{(u,u)}^H \in \mathbb{C}^{(N\times N)}$ by $\mathbf{y}^{(R)} \in \mathbb{C}^{(N\times 1)}$ in (13) is given by $(7N^2 - N)$ flops. Thus, the total complexity required for Algorithm 1 is given by

$$C_{TT} = \left(39N^2 + 23N + 28\right) \text{ flops.} \tag{32}$$

As a result, the total complexity required for signal estimate at R for SM-QSIC is given by

$$\begin{aligned} C_{\text{SM-QSIC}} &= N^2\left(C_{TT} + C_{\widehat{Q}(\cdot)} + C_{Q(\cdot)} + 20N + 38\right) \\ &\quad + 2C_{Q(\cdot)} + 31 = \left(39N^4 + 43N^3\right. \\ &\quad \left. + \left(C_{\widehat{Q}(\cdot)} + C_{Q(\cdot)} + 66\right)N^2 + 2C_{Q(\cdot)} + 31\right) \text{ flops.} \end{aligned} \tag{33}$$

The total complexity of SM-ML in [10, 12] calculated in (2) is given by

$$\begin{aligned} C_{\text{SM-ML}} &= N^2M^2(20N - 1) \\ &= \left(20N^3M^2 - N^2M^2\right) \text{ flops.} \end{aligned} \tag{34}$$

The total complexity for the EGA and EQRP method in [15] are estimated as follows:

$$\begin{aligned} C_{\text{EGA}} &= \left(N^4M + N^4(N - M) + \left(1 + N^2\right)\frac{M^3}{2}\right) \text{ flops,} \\ C_{\text{EQRP}} &= \left(N^4M + \left(1 + N^2\right)\frac{M^3}{2}\right) \text{ flops.} \end{aligned} \tag{35}$$

It is clear that the complexity of SM-ML [10, 12] and both EGA and EQRP in [15] depend mainly on the modulation order of the M-QAM constellation. Therefore, when the modulation order M is high, these methods do not achieve high efficiency compared to the proposed method.

Table 3: The sets of $\mathscr{B}$ according to M.

	$M = 4$	$M = 16$	$M = 64$
$\mathscr{B}$	$\{1+3j, 3+j\}$	$\{3+9j, 5+7j, 7+5j, 9+3j\}$	$\{7+21j, 9+19j, 11+17j, 13+15j, 15+13j, 17+11j, 19+9j, 21+7j\}$

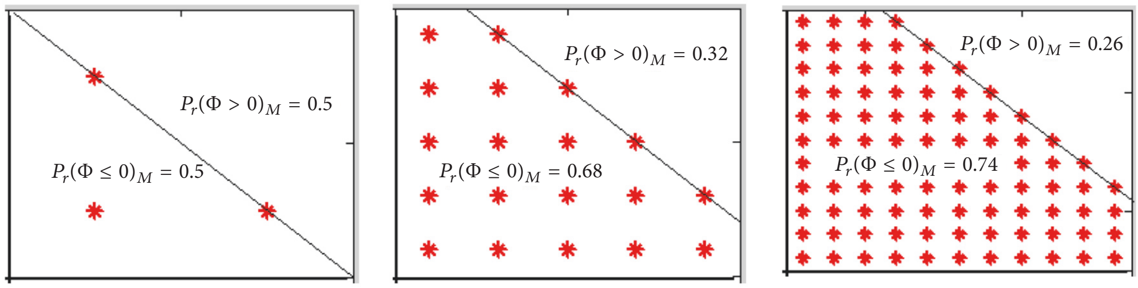

(a) $M = 4$ (b) $M = 16$ (c) $M = 64$

Figure 6: Probability that the estimation point lying on the left or the right of the boundary.

Table 4: The probability values $P_r(\Phi \le 0)_M$ and $P_r(\Phi > 0)_M$ according to M.

	$M = 4$	$M = 16$	$M = 64$
$P_r(\Phi \le 0)_M$	0.5	0.68	0.74
$P_r(\Phi > 0)_M$	0.5	0.32	0.26

Table 5: The values of $\mathscr{A}_{M,\overline{L}}$ and $\mathscr{B}_M$ according to M.

	$M = 4$	$M = 16$	$M = 64$
$\mathscr{A}_{M,\overline{L}}$	5/3	11/3	23/3
$\mathscr{B}_M$	2	4	8

Table 6: The complexity of functions $\widehat{Q}(\cdot)$ and $Q(\cdot)$ according to M flops.

	$M = 4$	$M = 16$	$M = 64$
$C_{\widehat{Q}(\cdot)}$	14.7	26.7	50.5
$C_{Q(\cdot)}$	2	16	29

5. Simulation Results and Performance Evaluation

This section presents simulation results of BER and complexities of different estimation methods. The simulation results of the proposed SM-QSIC method are compared with that of the ML estimation method in [10, 12] (denoted by SM-ML), the ML one in the conventional SIMO system (denoted by SIMO-ML), and the EGA, EQRD ones [15]. Let $V \times D \times V$ denote the system configuration, where V is the number of antennas of the terminal node and D is the number of antennas at the relay node.

For fair comparison, performance is evaluated at the relay for the proposed method and the SM-ML in [12]. Assume that the relay knows one of the two signals from the terminal nodes and that power of each node is equal to P, ($P_{T_1} = P_{T_2} = P_R = P$). Figures 7, 8, and 9 show the BER performances obtained at the spectral efficiency of 4 bps/Hz, 5 bps/Hz, and 6 bps/Hz. It can be seen that performance of the proposed method is close to that of the ML one [12] for the same spatial modulation configuration. Furthermore, the proposed method obtains higher SNR gain than the ML one in the SIMO system for the same transmission rate and the number of receive antennas at the relay. Particularly, at BER $= 10^{-3}$, the SM-QSIC offers about 4 dB SNR gain at the spectral efficiency of 4 bps/Hz, about 7.5 dB SNR gain at 5 bps/Hz, and about 5 dB SNR gain at 6 bps/Hz over the ML in the SIMO system. This SNR gain increases with SNR or N.

Next, we compare the end-to-end BER of the SM-QSIC and the ML [10]. For fair comparison, we assume that the transmit power of all terminals is the same and equal to half of the transmit power of the relay ($P_R = P$). Figures 10 and 11 compare the BER performances at the spectral efficiency of 4 bps/Hz and 6 bps/Hz. It can be seen that the proposed method outperforms the SIMO system without the spatial modulation. Particularly, at BER $= 10^{-3}$ and the spectral efficiency of 4 bps/Hz, the proposed method achieves about 7 dB SNR gain compared with the SIMO one. More SNR gain can be achieved at higher SNR or higher spectral efficiency. Compared with the ML method [10], the proposed one loses only about 0.7 dB SNR gain at low spectral efficiency (Figure 10) but achieves the same performance at high spectral efficiency (Figure 11).

The processing efficiencies in terms of flops/symbol of the related schemes are compared in Table 7. It can be clearly seen that the proposed SM-QSIC scheme has the complexity that depends only slightly on the modulation order M but more on the number of the transmit antennas N. Moreover, the proposed scheme has much lower complexity compared with that of the ML estimation in [10, 12], especially for high modulation order. Although it has higher complexity than the EGA and the EQRP in [15] for $M = 4$, the proposed scheme becomes much more effective for $M > 4$. Therefore, the proposed scheme is more suitable for high rate transmission systems.

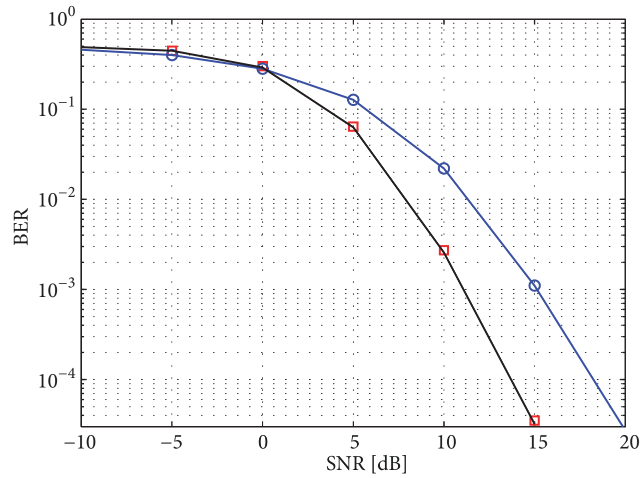

Figure 7: BER comparison at the spectral efficiency of 4 bps/Hz, with $N = 4$ and $M = 4$.

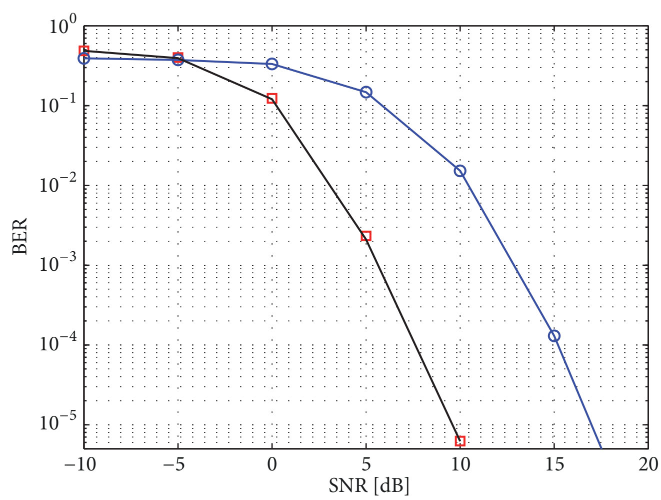

Figure 8: BER comparison at spectral efficiency of 5 bps/Hz, with $N = 8$ and $M = 4$.

Table 7: Processing efficiency comparison at the relay [flops/symbol].

Schemes	$N = 2$			$N = 4$		
	$M = 4$	$M = 16$	$M = 64$	$M = 4$	$M = 16$	$M = 64$
SM-ML [10, 12]	624	9.984	159.744	5.056	80.896	1.294.336
EGA [15]	48	2.568	163.848	392	8.960	55.7312
EQRP [15]	56	2.624	164.096	392	9.728	56.1152
Proposed SM-QSIC	334	367	410	3.524	3.635	3.789

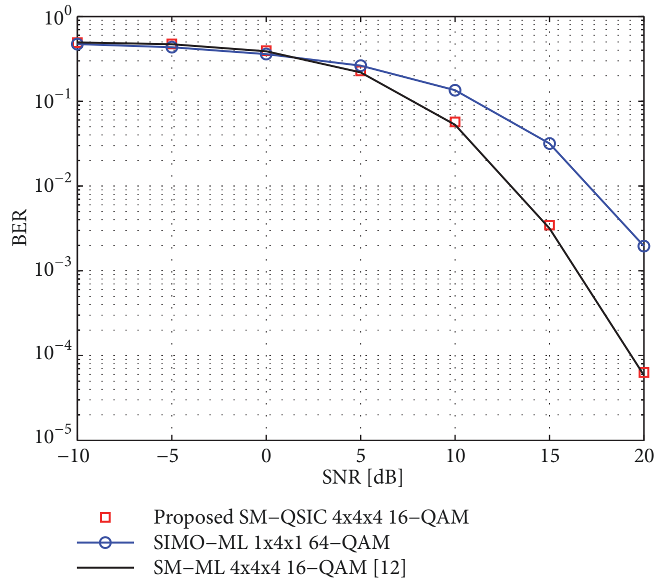

Figure 9: BER comparison at spectral efficiency of 6 bps/Hz, with $N = 4$ and $M = 16$.

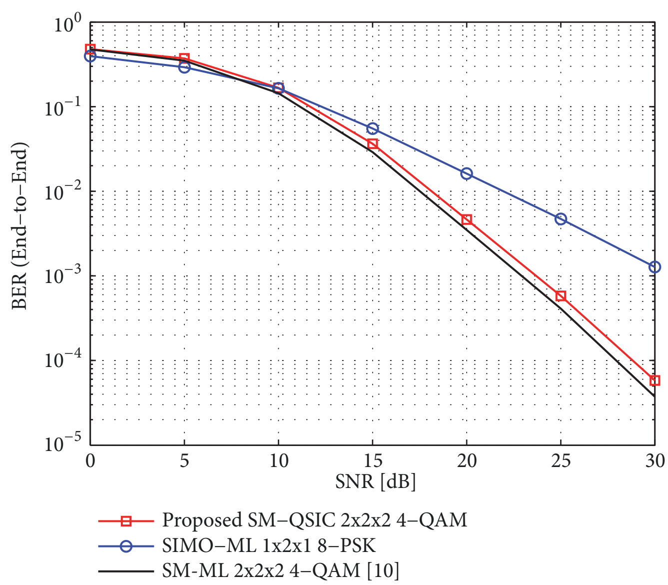

Figure 10: BER comparison from terminal to terminal at spectral efficiency of 3 bps/Hz, with $N = 2$ and $M = 4$.

6. Conclusions

This paper proposed a low-complexity estimation method using channel quantization and SIC for spatially modulated PNC systems. In our scheme, SIC was implemented first to estimate the activated antenna indices and then the modulated M-QAM symbol. We also designed signal constellations for the combined signal $(x^{(1)} + Lx^{(2)})$ and derived a decision function $\widehat{Q}(\cdot)$ which facilitated a reduced-complexity estimator at the relay for arbitrary M-QAM modulation. Using simulation results and complexity analysis we showed that the proposed scheme achieves near-optimal performance of the ML estimation while requiring less computational complexity. The proposed scheme is thus a prospective candidate for those applications which require low computational complexity such as IoT systems.

Data Availability

No data were used to support this study.

Conflicts of Interest

The authors declare that they have no conflicts of interest.

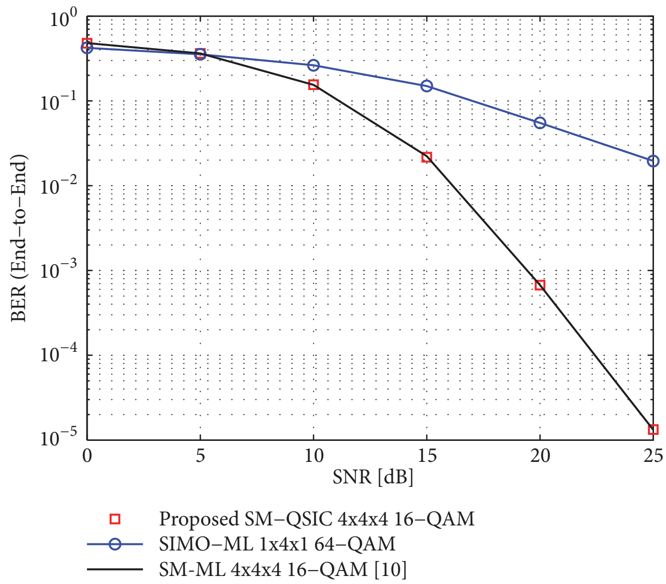

Figure 11: BER comparison from terminal to terminal at spectral efficiency of 6 bps/Hz, with $N = 4$ and $M = 16$.

Acknowledgments

This research is funded by Vietnam National Foundation for Science and Technology Development (NAFOSTED) under Grant no. 102.02-2015.23.

References

[1] L. Shi and S. C. Liew, "Complex linear physical-layer network coding," *Institute of Electrical and Electronics Engineers Transactions on Information Theory*, vol. 63, no. 8, pp. 4949–4981, 2017.

[2] K. Ravindran, A. Thangaraj, and S. Bhashyam, "High SNR Error Analysis for Bidirectional Relaying with Physical Layer Network Coding," *IEEE Transactions on Communications*, vol. 65, no. 4, pp. 1536–1548, 2017.

[3] Q. Huo, L. Song, Y. Li, and B. Jiao, "Source and physical-layer network coding for correlated two-way relaying," *IET Communications*, vol. 10, no. 5, pp. 502–507, 2016.

[4] S. Zhang, Q. F. Zhou, C. Kai, and W. Zhang, "Full diversity physical-layer network coding in two-way relay channels with multiple antennas," *IEEE Transactions on Wireless Communications*, vol. 13, no. 8, pp. 4273–4282, 2014.

[5] P. Popovski and H. Yomo, "Physical network coding in two-way wireless relay channels," in *Proceedings of the 2007 IEEE International Conference on Communications, ICC'07*, pp. 707–712, UK, June 2007.

[6] R. Y. Chang, S. Lin, and W. Chung, "On network coding and modulation mapping for three-phase bidirectional relaying," in *Proceedings of the 2015 IEEE 26th Annual International Symposium on Personal, Indoor, and Mobile Radio Communications (PIMRC)*, pp. 191–196, Hong Kong, China, August 2015.

[7] H. M. Nguyen, V. B. Pham, X. N. Tran, and T. N. Tran, "Channel quantization based physical-layer network coding for MIMO two-way relay networks," in *Proceedings of the 2016 International Conference on Advanced Technologies for Communications (ATC)*, pp. 197–203, Hanoi, Vietnam, October 2016.

[8] H. M. Nguyen, X. N. Tran, V. B. Pham, and T. N. Tran, "Channel quantization-based physical-layer network coding for two-way relay STBC system," *Vietnam Journal of Computer Science*, vol. 5, no. 1, pp. 59–66, 2018.

[9] R. Y. Mesleh, H. Haas, S. Sinanović, C. W. Ahn, and S. Yun, "Spatial modulation," *IEEE Transactions on Vehicular Technology*, vol. 57, no. 4, pp. 2228–2241, 2008.

[10] Y. Yang, "Spatial modulation exploited in non-reciprocal two-way relay channels: Efficient protocols and capacity analysis," *IEEE Transactions on Communications*, vol. 64, no. 7, pp. 2821–2834, 2016.

[11] K. G. Unnikrishnan and B. S. Rajan, "Space-time coded spatial modulated physical layer network coding for two-way relaying," *IEEE Transactions on Wireless Communications*, vol. 14, no. 1, pp. 331–342, 2015.

[12] B. C. Jung, J. S. Yoo, and W. Lee, "A practical physical-layer network coding with spatial modulation in two-way relay networks," *The Computer Journal*, vol. 61, no. 2, pp. 264–272, 2018.

[13] E. Chu, J. S. Yoo, and B. C. Jung, "Spatial-modulated physical-layer network coding in two-way relay networks with convolutional codes," in *Proceedings of the 2017 Ninth International Conference on Ubiquitous and Future Networks (ICUFN)*, pp. 811–813, Milan, July 2017.

[14] J. Zheng, "Hybrid Spatial Modulation Aided Distributed Relays: Threshold Detection and Constellation Rotation," *IEEE Access*, vol. 5, pp. 21242–21249, 2017.

[15] C.-T. Lin, W.-R. Wu, and C.-Y. Liu, "Low-complexity ML detectors for generalized spatial modulation systems," *IEEE Transactions on Communications*, vol. 63, no. 11, pp. 4214–4230, 2015.

[16] M. Higashinaka, K. Motoyoshi, T. Nagayasu, H. Kubo, A. Shibuya, and A. Okazaki, "Likelihood Estimation for Reduced-Complexity ML Detectors in a MIMO System," in *Proceedings of the 2007 IEEE 65th Vehicular Technology Conference*, pp. 2104–2108, Dublin, Ireland, April 2007.

[17] S. Zhang, Q. F. Zhou, C. Kai, and W. Zhang, "Channel quantization based physical-layer network coding," in *Proceedings of the 2013 IEEE International Conference on Communications (ICC)*, pp. 5137–5142, Budapest, Hungary, June 2013.

[18] C. W. Joon, C. K. Wui, and J. M. Cioffi, "Iterative soft interference cancellation for multiple antenna systems," in *Proceeding of the IEEE Wireless Communications and Networking Conference*, vol. 1, pp. 304–309, Chicago, USA, 2000.

[19] X. N. Tran, H. C. Ho, T. Fujino, and Y. Karasawa, "Performance comparison of detection methods for combined STBC and SM systems," *IEICE Transactions on Communications*, vol. E91-B, no. 6, pp. 1734–1742, 2008.